

Photon excitation of surface plasmons in diffraction gratings: Effect of groove depth and spacing*

C. E. Wheeler,[†] E. T. Arakawa, and R. H. Ritchie

Health Physics Division, Oak Ridge National Laboratory, Oak Ridge, Tennessee 37830

(Received 21 July 1975)

Experimental data for three gratings of different groove profile and spacing are presented together with calculations using a recently developed theory which predicts the probability for photon-to-surface-plasmon conversion in terms of the surface profile and dielectric function of the metal coating of the grating. Theory and experiment are in reasonable agreement and indicate that the magnitude of photon-to-surface-plasmon coupling increases with both increasing groove depth and decreasing groove spacing.

I. INTRODUCTION

The periodic "roughness" of diffraction gratings has been employed by many experimenters in the study of surface-plasmon excitation at air-metal boundaries. Teng and Stern¹ investigated the radiative decay of surface plasmons produced in a grating surface by electron bombardment as well as the absorption of *p*-polarized photons from a light beam specularly reflected from the same surface. Cowan and Arakawa² studied the effect on the surface-plasmon dispersion relation of different metal and dielectric coatings of the grating surface by monitoring the radiative decay of surface plasmons into the diffracted orders. But only recently has there appeared, in the works of Hutley,³ Hutley and Bird,⁴ and Pockrand,⁵ a systematic experimental investigation into the effects of groove profile on the absorption in grating surfaces of photons in the visible region.

Theoretical treatments of groove-profile effects divide roughly into two categories. In the first category are those which are basically extensions of Fano's theory of resonant excitation of surface waves⁶; these include the works of Hessel and Oliner,⁷ Jovičević and Sesnic⁸ (for a surface with infinite conductivity), and Häggglund and Sellberg⁹ who compared their calculations with experimental data. In the second are those which employ diffraction theory, notably the integral-equation approach of McPhedran and Waterworth¹⁰ for grating surfaces of infinite conductivity and extended by McPhedran and Maystre¹¹ for surfaces of finite conductivity.

Although the theoretical treatments in both categories can be considered "rigorous" to one degree or another, the procedures necessary to obtain numerical results are formidable, requiring the use of large computers with the significance of groove profile and dielectric parameters obscured by the numerical analysis. In contrast, the theoretical treatment with which our experimental data are compared is based on perturbation theory and requires rather sophisticated mathematics,

but the resulting expression for the probability of photon-to-surface-plasmon conversion is simple enough to permit calculation on small computers and clearly demonstrates the effect of surface parameters.

II. THEORY

Excitation of surface plasmons by photons requires the conservation of both energy and wave vector (or momentum) parallel to the surface. For a grating surface, wave vector conservation requires that the surface plasmon wave vector \vec{k}_{SP} and the component of the photon wave vector parallel to the surface $\vec{k}_p \sin \theta$ satisfy

$$\vec{k}_{SP} = \vec{k}_p \sin \theta + N\vec{g}, \quad (1)$$

with N a nonzero integer and \vec{g} a vector which is parallel to the surface but perpendicular to the grooves and of magnitude $2\pi/d$, where d is the groove spacing. Excitation occurs only for *p*-polarized photons when the plane of incidence (defined by \vec{k}_p and the normal to the surface) is perpendicular to the grooves; for this case \vec{k}_{SP} and $\vec{k}_p \sin \theta$ are collinear although they may be opposite in direction for negative N . A theoretical treatment by Elson¹² gives the probability for this excitation process as

$$P_0 = \sum_N \Delta_N, \quad (2)$$

with

$$\begin{aligned} \Delta_N = & 8\pi^2 \lambda^{-2} |\xi_N|^2 \epsilon_2 |1 - \bar{\epsilon}|^2 \cos \theta |2\sigma_N^2 - \bar{\epsilon}| \\ & \times |[(\sigma_N^2 - 1)(\sin^2 \theta - \bar{\epsilon})]^{1/2} - \sigma_N \sin \theta|^2 \\ & \times [\text{Re}(\sigma_N^2 - \bar{\epsilon})^{1/2} (\sin^2 \theta - \bar{\epsilon})^{1/2} - i \bar{\epsilon} \cos \theta]^2 \\ & \times |(\sigma_N^2 - \bar{\epsilon})^{1/2} + \bar{\epsilon}(\sigma_N^2 - 1)^{1/2}|^{-2}. \end{aligned} \quad (3)$$

ξ_N is the N th coefficient of the Fourier transform of the groove profile while λ is the wavelength of the incident photon, $\bar{\epsilon} = \epsilon_1 + i\epsilon_2$ is the dielectric function of the metal, and $\sigma_N = \sin \theta + N\lambda/d$. This expression was derived using a first-order perturbation treatment of the boundary value problem for

the magnetic vector potential \vec{A} , utilizing a transformation to relative coordinates and a dyadic Green's function; Elson and Ritchie¹³ employed similar techniques for a randomly rough surface, but used the Hertz vector potential instead of \vec{A} . The theory is applicable for metal surfaces only for the energy (or wavelength) region for which surface plasmons exist, that is for $\epsilon_1 < -1$. The wavelength region for which this is true varies from metal to metal, but for Al, ϵ_1 is large and negative from the infrared well into the vacuum ultraviolet with both ϵ_2 (always positive) and $|\epsilon_1|$ decreasing with λ .

Fundamental to the perturbation treatment is the assumption that the wavelength of the incident photon is much larger than the groove depth. In order to be able to use Eq. (2) when this approximation may not be satisfied, we have calculated the probability P of photon-to-surface-plasmon conversion as¹⁴

$$P = 1 - e^{-P_0}. \quad (4)$$

When using this expression, P never exceeds unity and reduces to P_0 when P_0 is small.

III. EXPERIMENT

As suggested by Hutley,³ grating efficiency is completely specified if it is measured as a function of angle of incidence for constant wavelength over the full range of wavelengths for which it is to be used. According to Eq. (1), fixing θ and scanning \vec{k}_p is completely equivalent to fixing \vec{k}_p and scanning θ . The former approach was adopted by Hägglund and Sellberg,⁹ and Bjork *et al.*,¹⁵ although it would seem to have the disadvantage that $\vec{\epsilon}$ changes with \vec{k}_p . Consequently, we used the latter approach, so that the experiment consisted of directing p -polarized monochromatic light onto a grating surface mounted in a reflectance chamber and recording the intensity of the specularly reflected beam as the grating was rotated. At an angle θ such that Eq. (1) was satisfied, a dip in reflectance occurred because energy was absorbed from the incident beam due to surface-plasmon excitation. The observed reflectance is thus equal to the ordinary reflectance of the surface (which exhibits a slow θ variation) minus P , so that the angular (θ) variation of the dips is that of P .

IV. CALCULATIONS

The wavelength of the incident photons was chosen so that the angular separation of dips in reflectance for different N was a maximum with the result that $1 - e^{-P_0}$ from Eq. (4) became $1 - e^{-\Delta N} \equiv P_N$. Since the maximum value of P_N corresponded to the minimum of the dip in reflectance, the convention was adopted of plotting P_N increasing downward. Calculations were performed

at 0.1-deg intervals and averaged over the beam divergence of approximately 0.4 deg. Although the experimental data which are presented are for Al-coated surfaces, preliminary calculations using published values of ϵ_1 and ϵ_2 for Al showed these values to be inappropriate. Published values of ϵ_1 and ϵ_2 are determined for Al surfaces prepared under high vacuum conditions; however, an Al surface oxidizes quickly when removed from the vacuum. The formation of an oxide layer on an Al surface has been shown to affect the surface-plasmon dispersion relation and the dielectric properties for that Al surface.² Furthermore, the surface-plasmon dispersion relation and damping have been shown to depend on the groove depth for Ag-coated grating surfaces.⁵ Although these effects should be smaller for an Al surface than for Ag,¹⁶ the magnitude of these effects cannot, at present, be treated theoretically. Consequently, these effects are combined into an "effective" dielectric function $\vec{\epsilon}$, determined from the experimental data. For a given photon wavelength, the angular positions of the minima of the theoretical dips ($\max P_N$) are determined by $|\epsilon_1|$; thus an effective $|\epsilon_1|$ is determined by angular coincidence of the experimental and theoretical dips. Similarly, requiring that the angular widths of the theoretical and experimental dips be equal determines an effective ϵ_2 . Finally, all calculations presented are for a triangular groove profile with base d , blaze angle α , and apex angle $\beta = 90^\circ$ as specified by the manufacturer. For a given photon wavelength, the relative magnitudes ($\max P_N$) of the theoretical dips depend only on the groove profile and are virtually independent of $\vec{\epsilon}$. Adjustment of groove profile parameters to shift the relative magnitudes of $\max P_N$ is straightforward, but to be reasonable, any adjustment of the parameters must produce agreement between the relative magnitudes of the theoretical and experimental dips in reflectance for all incident wavelengths; the need for a different profile for each λ would imply that the λ and θ dependence of Δ_N was wrong. Of course, the groove profile cannot be expected to be exactly triangular in the mathematical sense and probably varies somewhat from groove to groove and even within the same groove. But the assumption is made that the size of these variations is small compared to λ so that the "average" groove profile is basically triangular. It is further assumed that variations (such as rounded corners) are most likely to occur at the apex of the groove; thus, the blaze angle α is assumed to be most precisely defined with any uncertainty incorporated into the apex angle β . Since the relative magnitudes of $\max P_N$ depend on $|\zeta_N|^2$, it is noted that increasing β decreases $|\zeta_N|^2$ with respect to $|\zeta_{\alpha 1}|^2$, while decreasing β has the opposite effect, with the ratio

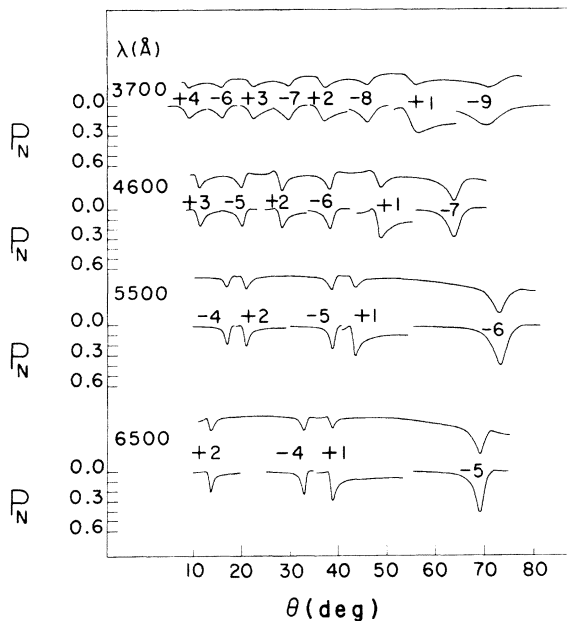


FIG. 1. Experimental reflectance (upper curve for each λ) and theoretical excitation probability (P_N) vs angle of incidence for grating A (600 grooves/mm, $\alpha = 2^\circ 35'$). Integers indicate appropriate N for each dip.

$|\xi_N|^2/|\xi_{+1}|^2$ being a maximum for $\alpha + \beta = 90^\circ$ (one groove facet vertical).

V. RESULTS AND DISCUSSION

Figure 1 gives the experimental reflectance¹⁷ and theoretical excitation probability P_N for grating A. This grating has 600 grooves/mm and a blaze angle of $2^\circ 35'$ so that the groove depth is much smaller than the shortest wavelength investigated. Perturbation theory would be expected to hold well for this groove profile. Indeed, the calculations are seen to agree well with the experimental reflectance. These curves illustrate several of the general features of both the experimental and calculated reflectance. First, for constant λ (and thus constant ξ) both the depth ($\max P_N$) and angular half-widths of the dips tend to increase with θ . Secondly, as λ decreases, dips for a given N become broader and more shallow; this is due to the usual variation of ξ with λ . Third, the θ variation of the dips for positive N is opposite to that for the dips with negative N ; that is, dips for positive N have steep slopes on the small θ side of the minimum and more gradual slopes on the large θ side, while the opposite θ variation is exhibited by dips for negative N . Finally, it is noted that as λ increases, dips for positive N occur at progressively smaller θ values while those for negative N move toward large θ values and increase in depth with respect to the other dips. Although the

theoretical calculations and experimental data are in substantial agreement for this surface, there is a slight discrepancy between the relative magnitude of $\max P_{+1}$ and $\max P_N$ and the relative magnitudes of the experimental dips. For example, at $\lambda = 5500 \text{ \AA}$ the magnitude of the experimental dip for $N = -5$ is larger than the magnitude of the dip for $N = +1$, whereas $\max P_{+1}$ is larger than $\max P_{-5}$, which indicates that $|\xi_{+1}|^2/|\xi_{-5}|^2$ is smaller for the actual profile than for the assumed profile. The ratio $|\xi_{+1}|^2/|\xi_N|^2$ can, in principle, be decreased by decreasing β , but full agreement between theory and experiment could not be achieved since β (and thus $|\xi_{+1}|^2/|\xi_N|^2$) for the assumed profile was very close to the minimum value already. A further decrease in the ratio $|\xi_{+1}|^2/|\xi_N|^2$ requires either the assumption, for example, of a flat space between the grooves or of a profile which is not strictly triangular. Investigation is continuing into the effect of nontriangular profiles on $\max P_N$ and also into which profile may represent the most "reasonable" approximation to the actual profile.

Figure 2 gives the experimental reflectance and excitation probability P_N for grating B. This grating has 1200 grooves/mm and a blaze angle of $5^\circ 10'$, so that its groove depth is the same as for grating A, whereas its groove spacing is only half as large. Aside from the fact that there are fewer

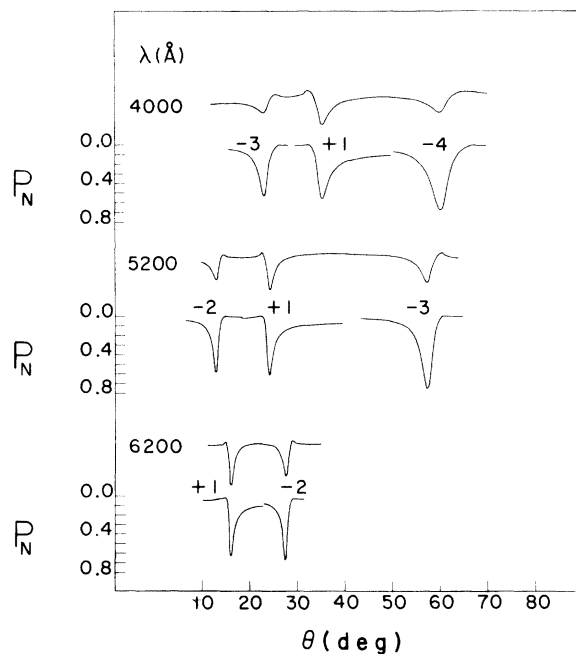


FIG. 2. Experimental reflectance (upper curve for each λ) and theoretical excitation probability (P_N) vs angle of incidence for grating B (1200 grooves/mm, $\alpha = 5^\circ 10'$). Integers indicate appropriate N for each dip.

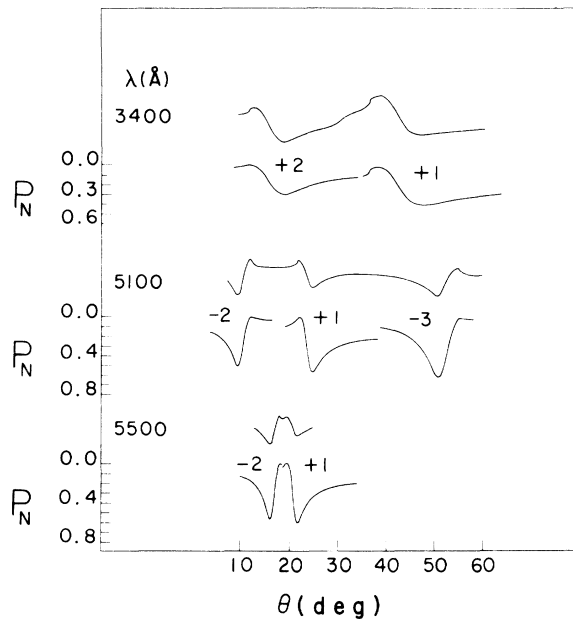


FIG. 3. Experimental reflectance (upper curve for each λ) and theoretical excitation probability (P_N) vs angle of incidence for grating C (1200 grooves/mm, $\alpha = 7^\circ 7'$). Integers indicate appropriate N for each dip.

dips for a given λ due to the increase in \vec{g} (decrease in d), the experimental and theoretical curves in Fig. 2 show much the same λ and θ dependence as do those in Fig. 1. The experimental dips in reflectance for grating B are much stronger and of larger angular extent than those for grating A, indicating a larger probability for photon-to-surface-plasmon conversion, even though the groove depths (and thus $|\zeta_{+1}|^2$) are approximately the same. The calculations are not in complete agreement with the experimental reflectance, since the magnitudes $\max P_N$ of the calculated dips are larger relative to $\max P_{+1}$ than are the corresponding magnitudes of the experimental dips. This suggests that $|\zeta_{+1}|^2/|\zeta_N|^2$ is larger for the actual groove profile than for the assumed profile. This ratio can be increased by increasing the apex angle β ; in fact, the relative magnitudes of the experimental and theoretical dips agree exactly if β is taken to be 145° to 150° . Even with these profile parameters, the magnitudes of the theoretical dips are much larger for grating B than for grating A, supporting the assertion that the probability of photon-to-surface-plasmon conversion increases with decreasing groove spacing (for constant groove depth).

Figure 3 gives the experimental reflectance and the theoretical excitation probability P_N for grating C which has 1200 grooves/mm and blaze angle of $7^\circ 7'$, so that the groove depth is approximately 1025 \AA . The broader dips in reflectance for this

grating indicate stronger photon-to-surface-plasmon coupling over a larger angular extent than for grating B. The data of Hutley³ for Al and of Pockrand⁵ for Ag exhibit the same variation with groove depth. At $\lambda = 3400 \text{ \AA}$, the broad dips which extend over 20° to 30° for this grating are in sharp contrast to the deep, narrow dips for gratings A and B; reproduction of such a wide variety of dips with such diverse shapes illustrates the versatility of the theory and the sensitivity of surface-plasmon excitation to $\vec{\epsilon}$. Theoretically, the dips for grating C should be deeper and slightly broader than those for grating B, since the increase in groove depth means an increase in $|\zeta_N|^2$ which increases P_N by a scale factor. Actually, the increase in $\max P_N$ from the increase in groove depth is partially negated by an increase in damping as discussed below. Thus, the theory also indicates that the probability of photon-to-surface-plasmon conversion increases with groove depth for constant groove spacing. As can be seen in Fig. 3, for $\lambda = 5100$ and 5500 \AA the magnitudes $\max P_{+1}$ are larger relative to $\max P_{-2}$ than is found experimentally; this is basically the same situation as for grating A and could not be resolved without resorting to a groove profile that was not strictly triangular.

Summarized in Table I are the values of ϵ_1 and ϵ_2 determined for gratings A, B, and C. Listed for reference are ϵ_1 and ϵ_2 calculated from the published data of Hunter,¹⁸ Schultz,¹⁹ and Schultz and Tangherlini²⁰ and an estimate²¹ of ϵ_1' for an Al surface coated with a 50-\AA layer of oxide. For grating A, ϵ_1 is fairly close to ϵ_1' ; $|\epsilon_1|$ and ϵ_2 are slightly smaller for grating B compared to grating A. Pockrand⁵ has suggested that the increase in angular width of the dips in reflectance with increasing groove depth was due to stronger radiative damping of the surface plasmons. This increase in damping is manifested for grating C as a substantial increase in ϵ_2 with respect to $|\epsilon_1|$.

VI. CONCLUSIONS

The probability for surface-plasmon excitation in grating surfaces has been shown to increase with increasing groove depth by comparing data for gratings with the same groove spacing and to increase with decreasing groove spacing by comparing data for gratings with the same groove depth. Theoretical excitation probabilities obtained by fitting the Elson-Ritchie theory to the experimental reflectance substantiates this conclusion. The validity of this theory has been confirmed for two grating surfaces with groove profile parameters which satisfy the assumptions of the perturbation treatment. Furthermore, this theory has been shown to give reasonable agreement for a grating whose surface parameters may

TABLE I. Dielectric functions for smooth Al surfaces, for smooth Al surface with 50-Å oxide layer, and for gratings A, B, and C.

λ (Å)	Hunter		Schultz and Tangherlini		ϵ_1' for 50-Å oxide layer	Grating A		Grating B		Grating C	
	ϵ_1	ϵ_2	ϵ_1	ϵ_2	ϵ_1	ϵ_1	ϵ_2	ϵ_1	ϵ_2	ϵ_1	ϵ_2
3400										-4.3	2.6
3500	-16.3	2.8			-10.1						
3700						-10.0	3.2				
4000	-21.0	4.0	-15.2	3.1	-13.1			-9.8	2.5		
4100						-12.9	3.6	-10.4	2.7	-6.8	3.8
4200								-11.0	2.9	-7.9	4.1
4500	-25.7	5.5	-18.4	4.2	-16.3	-14.7	4.7				
4600						-16.4	5.3				
4700								-13.1	3.8		
4800								-14.2	4.0		
4900								-14.5	4.1	-9.2	5.4
5000	-33.2	8.1	-22.7	6.0	-20.7			-15.3	4.2		
5100						-19.3	6.2	-16.1	4.4	-10.8	6.1
5200								-16.9	4.7		
5300								-17.7	5.1		
5400						-21.6	7.0	-18.1	5.6		
5500	-37.8	10.3	-27.7	8.1	-24.8	-22.5	7.2	-19.4	5.8	-13.2	7.1
6000	-48.7	13.8	-35.1	11.6	-31.6			-20.7	6.4		
6200						-26.8	8.9	-22.6	6.7		
6500			-42.0	16.4		-30.0	10.0				

not strictly satisfy these assumptions. In fact, this theory can reproduce a wide variety of dips in reflectance with the use of appropriate values of the dielectric function, illustrating the dependence of surface-plasmon excitation on this function. Finally, the compactness of the final ex-

pression for P_N facilitates the determination of $\bar{\epsilon}$ from fitting the theory to the experimental data which represents a significant advantage over previous theories in which the significance of surface structure and dielectric parameters is obscured by the mathematics.

*Research sponsored by the Energy Research and Development Administration under contract with Union Carbide Corp.

†Present address: University of Tennessee, Knoxville, Tenn.

¹Y. Y. Teng and E. A. Stern, Phys. Rev. Lett. **19**, 511 (1967).

²J. J. Cowan and E. T. Arakawa, Phys. Status Solidi A **1**, 695 (1970); Z. Phys. **235**, 97 (1970).

³M. C. Hutley, Opt. Acta **20**, 607 (1973).

⁴M. C. Hutley and V. M. Bird, Opt. Acta **20**, 771 (1973).

⁵I. Pockrand, Phys. Lett. A **49**, 259 (1974).

⁶U. Fano, J. Opt. Soc. Am. **31**, 213 (1941).

⁷A. Hessel and A. A. Oliner, Appl. Opt. **4**, 1275 (1965).

⁸S. Jovičević and S. Sesnic, J. Opt. Soc. Am. **62**, 865 (1972).

⁹J. Häggglund and F. Sellberg, J. Opt. Soc. Am. **56**, 1031 (1966).

¹⁰R. C. McPhedran and M. D. Waterworth, Opt. Acta **19**, 877 (1972); **20**, 177 (1973); **20**, 533 (1973).

¹¹R. C. McPhedran and D. Maystre, Opt. Acta **21**, 413 (1974).

¹²J. M. Elson (private communication).

¹³J. M. Elson and R. H. Ritchie, Phys. Status Solidi B **62**, 461 (1974).

¹⁴J. M. Elson and R. H. Ritchie, Oak Ridge National Laboratory, Report No. ORNL-TM-3752 (1972) (unpublished).

¹⁵R. H. Bjork, Y. Y. Teng, and A. S. Karakashian, Phys. Lett. A **37**, 27 (1971); Phys. Rev. B **9**, 1394 (1974).

¹⁶It is shown in Ref. 5 that the magnitude of these effects increases with $|\vec{K}_{sp}|$; for a given energy, $|\vec{K}_{sp}|$ is larger for Ag than for Al.

¹⁷These data are representative of the general λ variation of the reflectance, although these specific wavelengths were chosen to facilitate the theoretical calculations.

¹⁸W. R. Hunter, J. Phys. (Paris) **25**, 154 (1964).

¹⁹L. G. Schultz, J. Opt. Soc. Am. **44**, 357 (1954).

²⁰L. G. Schultz and F. R. Tangherlini, J. Opt. Soc. Am. **44**, 362 (1954).

²¹C. E. Wheeler, Ph.D. thesis (University of Tennessee, 1975) (unpublished).